

## Supporting Information

# Synthesis of graphitic mesoporous carbon from sucrose as catalyst support for ethanol electro-oxidation

Dingsheng Yuan\*, Xiaoli Yuan, Wujun Zou, Fulong Zeng, Xiangjin Huang, Shuangli

Zhou

Department of Chemistry, Jinan University, Guangzhou 510632, P.R.China

E-mail: tydsh@jnu.edu.cn

The small angle X-ray diffraction patterns of MFe and GMC do not display (100), (110) and (200) reflections, indicating that the MFe and GMC are not completely duplicated the long range order of SBA-15.

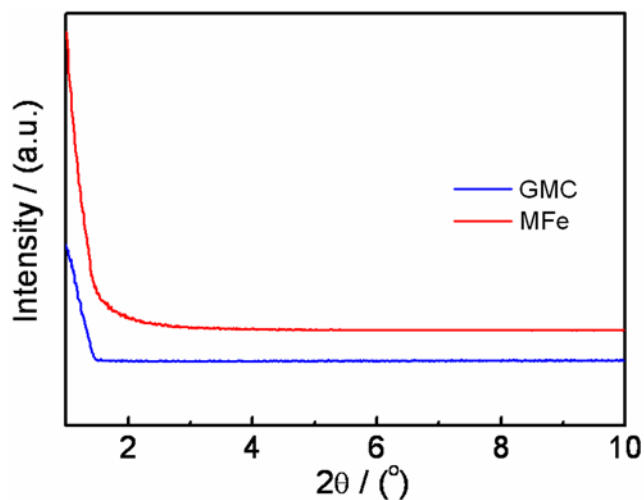


Fig.S1 The small angle X-ray diffraction patterns of MFe and GMC

In this study, a disordered mesoporous carbon was obtained, which can also be proved by the TEM analysis. The disordered mesopores of the GMC are clearly observed in Fig. S2a, which is in good agreement with the small angle X-ray diffraction patterns. The (002) lattice fringes of graphitic structure and microporous carbon are clearly observed in HRTEM image (see Fig. S2b).

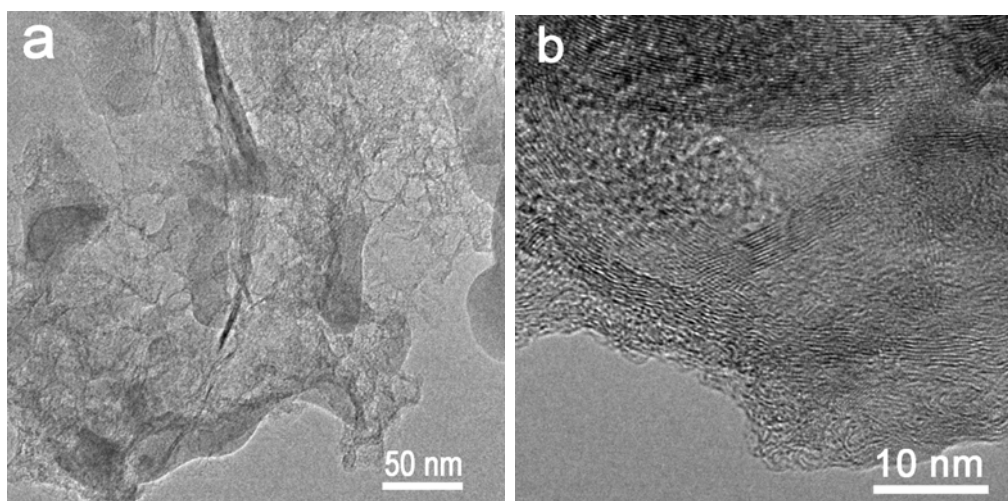


Fig.S2 The HRTEM images of GMC.

Fig.S3 shows the compared Raman spectra. The sharp D band indicates disordered C and defect in GMC. Meanwhile, the 2D-band peak of GMC is clearly observed in the spectrum, suggesting that the GMC had highly graphitic degree than XC-72 and CMK-3. These are all accordance with the TEM measurements.

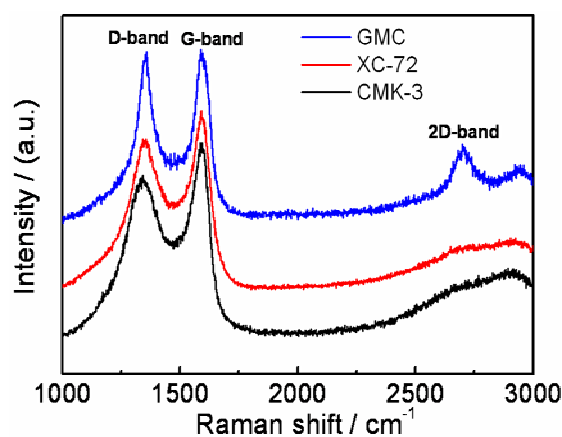


Fig. S3 Raman spectra of the GMC and XC-72.

The  $\pi$  and  $\sigma$  peak of GMC is characterized by XPS spectra different from carbon black XC-72. C1s XPS spectra of GMC and XC-72 and the content of carbon types in different oxygen-containing functional groups can be seen in Fig. S4 and Table S1. As can be seen, the  $sp^2$  of GMC is up to 79.36 %, which is much higher than that in XC-72. Moreover,  $sp^3$  in XC-72 is 29.30%, implying that XC-72 contains more  $\sigma$  bonds. This suggests that degree of graphitization of the GMC is higher than XC-72 and it is well-known that graphitic carbon materials can show a higher resistance to carbon corrosion and more stable than amorphous carbon materials.

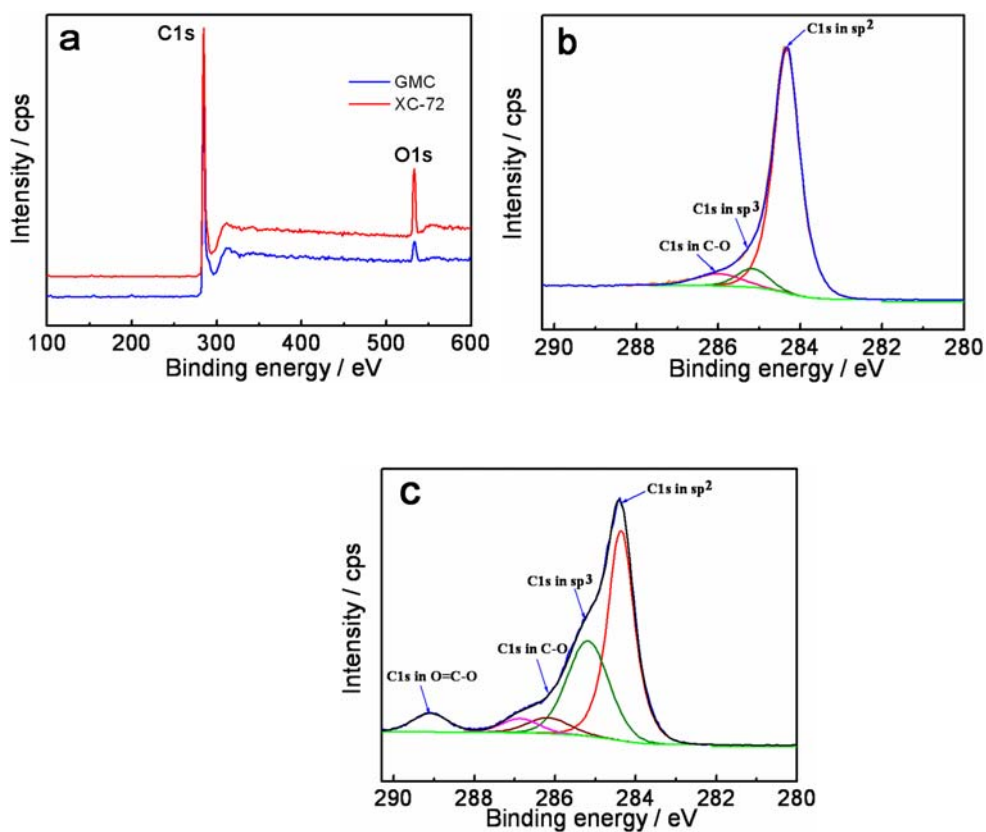


Fig. S4 The XPS wide spectra (a), C1s fine spectra of the GMC (b) and XC-72 (c) sample.

Table S1 The content of carbon types in different oxygen-containing functional groups.

Sample	C in sp <sup>2</sup> 284.3eV	C in sp <sup>3</sup> 285.2eV	C-O 286.0eV	O=C-O 289.1eV	C=O 286.9eV	O 1s 532.8eV
GMC	79.36	6.87	6.37	-	-	6.12
XC-72	45.01	29.30	4.89	4.94	3.94	11.93

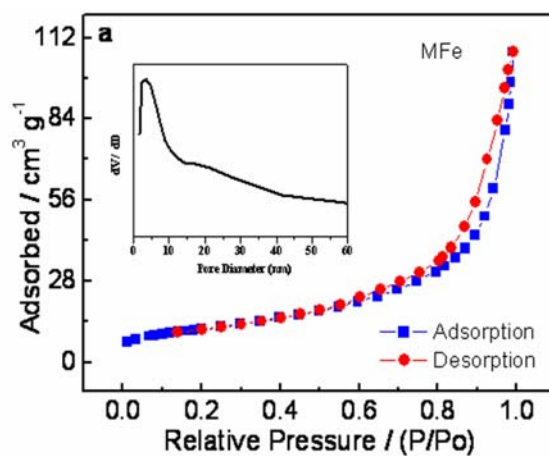


Fig. S5 Nitrogen sorption isotherm of MFe

The BET surface area and the corresponding pore size distribution curves for Pt/GMC, Pt/XC-72 and Pt/CMK-3 are shown in Fig. S6. As listed in Table S2, the pore parameters and specific surface area of Pt-loaded materials are smaller than those of carbon supports.

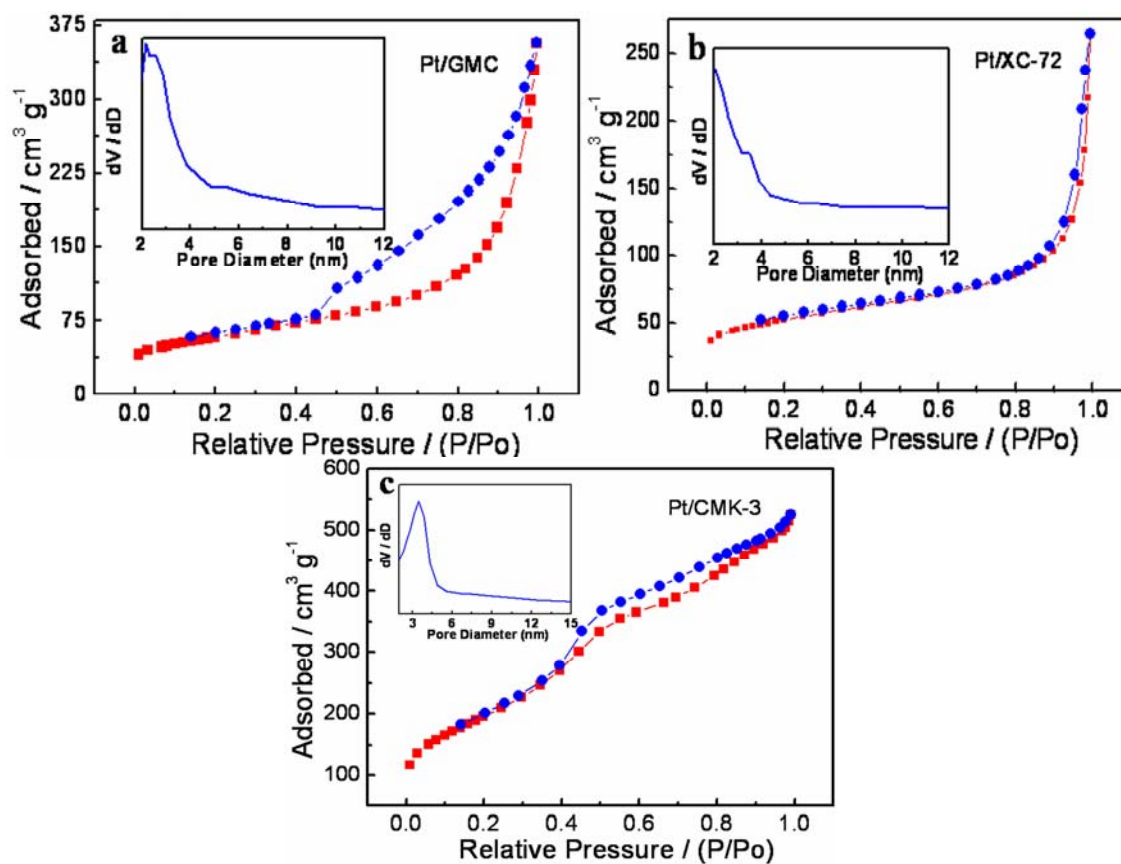


Fig. S6  $N_2$  adsorption-desorption isotherm and pore size distribution of Pt/GMC (a), Pt/XC-72 (b) and Pt/CMK-3

(c)

Table S2 Pore parameters and BET data of the materials

Sample name	$S_{BET}$ ( $m^2 g^{-1}$ )	$D$ (nm)	Pore volume ( $cm^3 g^{-1}$ )
Pt/GMC	206	2.2	0.43
GMC	232	3.6	0.82
Pt/XC-72	185	5.2	0.24
XC-72	246	5.9	0.36
Pt/CMK-3	708	3.5	0.77
CMK-3	1303	3.9	1.49